Supplementary Note 1. Dynamics of fluorescence transients in response to sustained depolarizations.

The relaxation of the quenching response observed for large, extended depolarizations could result from at least two processes: 1) a decrease in FRET between DPA and DiO and 2) a decrease in homoFRET between DiO molecules. Interestingly, the eGFP-F/DPA FRET pair also displays slight relaxations during 40 ms voltage pulses and slight overshoots in the tail fluorescence (**Fig. 1B, Supplementary and 5**). This implies that a component of the rebound and relaxation may be attributed to DPA. One possibility is that large voltage changes alter the ability of DPA to quench DiO fluorescence due either to changes in the local environment, increasing the effective distance between the molecules, or to changes in the relative rotation of the molecules' dipoles. Similar phenomena have been suggested to account for the behavior of the membrane staining dye merocyanine 540 (Dragsten and Webb, 1978).

We also considered the possibility that DiO itself might translocate between membrane leaflets in response to changes in membrane potential with a slower time course, and in this way contribute to the relaxation. Voltage dependent changes in fluorescence have been described previously for DiO-related carbocyanine dyes (Sims et al., 1974; Waggoner, 1976; Kimmich et al., 1977; Melikyan et al., 1996). In some of these experiments, slow (minutes) DiO fluorescence responses to membrane potential hyperpolarization are thought to be due to dye redistribution between the inside of the cell and the cell medium (Waggoner, 1976). Other fluorescence quenching (Dragsten et al., 1981) and voltage-clamp experiments (Melikyan et al., 1996), show that DiI-C_{16} and DiI-C_{18} have access to the inner leaflet of phospholipid cell bilayers.

In order to address whether DiO movement, on a time scale of tens of milliseconds, might contribute to the slow relaxation of the quenched signal during sustained depolarization we examined changes in DiO fluorescence in the absence of DPA (**Supplementary Fig. 4A**). We observed small increases in fluorescence upon step depolarization from -70 mV to +100 mV, similar to those reported for related carbocyanine dyes (Sims et al., 1974; Kimmich et al., 1977; Melikyan et al., 1996). On average the fluorescence changes were small (3.5 ± 0.6% $\Delta F/F$ per 100 mV, n=7) and slow (τ=41 ± 8 ms, n=6) in the absence of DPA **(Supplementary Fig. 4A)**. Although there may be other explanations, these data are consistent with a relief of homo-FRET, which has been demonstrated for DiO using anisotropy measurements (Sengupta et al., 2007), upon depolarization when cationic DiO molecules move from inner to outer membrane leaflet (Melikyan et al., 1996). If this were the case, sustained depolarization to potentials greater than ~0 mV would lead to a repartitioning of DiO predominantly to the outer leaflet. Such DiO repartitioning could increase fluorescence both by reducing DiO/DPA FRET and by reducing DiO self-quenching (see diagram in **Supplementary Fig. 4B**). This scenario provides an explanation for the relaxation and overshoot phases of response to extended, large depolarization.

As a test of the schematic model proposed in **Supplementary Figure 4**, we asked whether the initial holding potential can affect the voltage-dependent FRET response by examining the amplitude of the fast, DPA mediated, component of fluorescent change. We found that, regardless of whether eGFP-F labeled cells were stepped to -100 mV and +100 mV from a holding potential (HP) of -70 mV (**Supplementary Fig 5A,** black trace, bottom left panel), or from a holding potential of 0 mV (**Supplementary Fig 5B,** black trace, bottom right panel), the same total difference in $\Delta F/F$ was observed (about 20%), as would be expected from the large dynamic range of the voltage- dependence of the fluorescence due predominantly to DPA movement (Chanda et al., 2005). In contrast, when the same experiment was performed with DiO labeled cells we found 20% quenching for a jump from a HP of 0 mV compared to >50% quenching for the jump from a HP_t of -70 mV (**Supplementary Fig. 5A & B,** compare amplitudes of fast components in black traces, upper panels). This lack of linearity is also predicted from the voltage-dependence of the peak quenching amplitude in (Fig. 1C and Fig. 2) which indicates that below -80 mV and above +25mV the DiO/DPA quenching response is non-linear. When holding at 0 mV, a slow increase in fluorescence is evident during the depolarization step (**Supplementary Fig 5B upper, black trace),** which we attribute to DiO repartitioning to the outer leaflet (illustrated in the cartoon of panel number 3, **Supplementary Fig. 4B**). These data suggest that at strongly depolarized potentials DiO moves in response to voltage, and at steady state this redistribution curtails the amplitude of the fast DiO/DPA response. This process only occurs in response to large sustained potential changes outside of the physiological membrane potential range and is much slower than neuronal APs.

Supplementary Note 2: Factors affecting sensitivity: the presence of a pinhole, the signal to noise ratio, and the effectiveness of membrane labeling

Although the sensitivity ($\Delta F/F$ per 100 mV) increased under confocal detection in the presence of the pinhole, the decreased photon flux from the smaller detection volume (<0.25 μm^3) decreased the SNR from 6.0 to 2.5 **(Supplementary Figure 6,** compare left two traces). On average, the DiO/DPA FRET pair produced 23 ± 2% in non-confocal mode (n=7; SNR =7.2 ± 0.7) and 34 ± 3% $\Delta F/F/100$ mV (n=3; SNR = 2.9±1.0) using confocal detection. The increased sensitivity in this case likely results from reducing the contribution of photons from labeled structures that do not exhibit a stimulus dependent change in fluorescence outside the principle plane of focus. These findings indicate that in neurons under conditions in which AP properties are minimally perturbed by DPA (1 μM), the intrinsic sensitivity of the DiO/DPA FRET pair is large, as was the case for HEK-293 cells (**Figs. 1, 2 and 3**). In addition the results demonstrate that this FRET pair can be used with confocal detection to report the membrane potential from small cellular compartments.

Maximal ΔF/F values and SNR are sensitive to several factors including the degree to which fluorescence arises exclusively from the membrane, minor contaminating sources of fluorescence, and detection methodology. For example, the small differences between the mean ΔF/F per 100 mV of AP from cultured hippocampal neurons (-24% ΔF/F per 100 mV in 1 μM DPA) versus Purkinje neurons in slices (-19% ΔF/F per 100 mV) may in part be due to a slightly larger degree of cytoplasmic staining arising as a consequence of the cell-attached patch loading method used for the slice experiments (the majority of the hippocampal culture experiments were stained using bath application, which produces less cytoplasmic staining). In addition, we observed a reduction in Purkinje cell membrane staining over tens of minutes which we attribute to diffusion of DiO through the remaining Purkinje neuron cell surface after the finite labeling period, and/or to membrane internalization. SNR in the slice experiments may also be reduced by autofluorescence of the slice (which is not present in primary cultures), and the larger bandwidth necessary (3.5 kHz vs 1-2 kHz) for the rapid Purkinje cell transient. Finally, as with other optical methods, SNR increases can be gained by either increasing the illumination spot size or averaging over several pixels of a rapid CCD camera (e.g. (Djurisic et al., 2004)). Staining methods such as DiOlistics (Gan et al., 2000; O'Brien and Lummis, 2006) or *in vivo* tract labeling (Ratzliff et al., 2004) may improve SNR particularly if they favor plasma membrane staining relative to intracellular membrane staining.

Supplementary Figure 1. Illustration of raw DiO/DPA fluorescence decay correction. Raw fluorescence traces in a voltage clamped HEK 293 cell labeled with DiO-C_{16}, and in the presence of 1 μM DPA. The AOTF was triggered to allow 488 nm laser light to enter the microscope producing an increase in fluorescence relative to no illumination (dashed line). Fluorescence is in arbitrary units. **Blue trace** is without any stimulus and the **black trace** is with a depolarization using an AP waveform. After the rapid onset of illumination, the fluorescence decreased over two components. A double exponential fit (**grey trace**) of the trace without stimulus produced time constants of 1.7 and 16 ms, with relative amplitudes of 0.79 and 0.21, respectively. In order to correct for the fluorescence decay, the fit was then subtracted from traces with stimulus.

Supplementary Figure 2. Labeling of cells by cell-attached patch pipette method.
A and **C**, DIC, and **B** and **D**, fluorescent images of a HEK-293 cell before suction was applied through a patch pipette containing DiO-C_{16} (**A** and **D**), and after 15 seconds of suction was applied and the pipette backed away (**C** and **D**).

Supplementary Figure 3. DiO/DPA produces little fluorescence excitation-dependent toxicity. A, baseline fluorescence (filled circles) and leak current (filled triangles) from a voltage clamped (-70 mV), DiO labeled HEK cell in 1 μM DPA. Each trial consisted of an exposure to laser

illumination for 180 ms. The fluorescence amplitude and leak current were estimated from a time averaged (2 ms) amplitude 15 ms after the start of laser illumination. Each trial was interleaved with 1000 Hz trains of 10 x 0.5 ms duration depolarizing pulses (to +30 mV). **B,** baseline fluorescence (filled circles) and leak current (filled triangles) of the same cell as in A, but after another 130 trials in which the cell was illuminated as in A and stimulated (interleaved) with 10 x 1 ms pulses. The stimulus protocol used here was the same as in A. **C,** is the ΔF/F amplitude of the DiO/DPA fluorescence response of the first depolarizing pulse of individual trials. **D,** is similar to C, but after 231 previous trials. In both cases the ΔF/F amplitude is very stable during the 1.5s interval stimulation protocol (30 trials). **E,** shows averaged traces (17 sweeps) with (black) and without (grey) train depolarizations. **F,** similar to E, but after 231 previous trials (average 15 sweeps). **G,** superimposed averaged traces from E and F, converted to ΔF/F. Over the intervening 130 stimuli, there was only a moderate decrement in the baseline fluorescence (which could be due to small drifts of the preparation), and only a minor decrement in the ΔF/F response. We did not determine whether the increase in leak current observed between those trials of A versus those in B was caused by illumination, although it did not increase within the 50 seconds of contiguous trials in epochs A or B.

Supplementary Figure 4A. DiO labeled HEK-293 cells show an increase in fluorescence in response to step depolarizations.

Upper four panels, schematic diagram describing our interpretation of DiO fluorescence changes at different times (numbers) during a step depolarization (thick red line) in the absence of DPA. **Grey symbols** represent membrane phospholipids, **large green symbols** represent DiO molecules. **Arrows** represent 488 nm excitation (**blue**) and DiO emission (**green**). The length of the green arrows represents the amount of relative fluorescence emitted at the time indicated by the number. **Lower two panels,** Fluorescence signals in response to voltage steps (above), from a HEK-293 cell labeled with DiO_{16}, and patch-clamped in whole-cell mode at a holding potential of -70mV. Traces are averages of 50 sweeps per step (step duration = 80 ms) and filtered to (2000 point binomial smoothing, Igor Pro, Wavemetrics; <0.5 kHz equivalent Bessel filtering). Single exponential fits (grey) to the rising and falling phase of the +100 mV step (black trace) produced time constants of 48 and 17 ms, respectively.

Supplementary Figure 4B. Schematic diagram outlining DiO/DPA FRET responses to a step depolarization

Upper four panels, schematic diagram describing our interpretation of DiO fluorescence changes at different times during a step depolarization in the presence of DPA. Dynamic changes in DiO

fluorescence during sustained step depolarizations (from -70 mV to > 0 mV) result predominantly from a rapid repartitioning of DPA molecules to the inner leaflet (fluorescence quenching) followed by a slower repartition of DiO molecules (relaxation of quenching). Symbols are as in Supplementary Figure 4A, with the red symbol here representing DPA molecules. **Lower panel,** Fluorescence signal from a voltage-clamped HEK-293 cell labeled with DiO_{16} in the presence of 1 μM DPA in response to a step depolarization from -70 mV to +100 mV (above). Numbers correspond to the approximate time represented in the voltage command in the upper panels. Double exponential fit (solid grey) to the +100 mV pulse is 1.5 and 17 ms with relative amplitudes of 0.46 and 0.54, respectively.

Supplementary Figure 5. DiO fluorescence increases with a slower time course in response to large depolarizations

Fluorescence responses to step command potentials (upper panels) from a HEK-293 cell labeled with DiO_{18} (middle panels) or expressing eGFP-F (bottom panels), patch-clamped in whole-cell mode, and incubated with 5 μM DPA. Holding potentials were for **A**, -70 mV**,** or **B**, 0 mV. Voltage steps were to -100 mV, -5 mV, and +100 mV. Traces are averages of 7 (DiO, -70mV), 6 (DiO, -0mV), 14 (eGFP-F, -70mV), and 19 (eGFP-F, -0mV) sweeps per voltage step and were filtered to 1 kHz.

Supplementary Figure 6. DiO/DPA detection of action potentials from confocal volume. A, confocal image of a DiO_{16}-labeled cultured hippocampal neuron in the presence of 1 μM DPA. **Green circle** indicates location of recordings shown in **B**. **B**, averaged DiO/DPA fluorescence transient recorded without, **left,** (n= 10 sweeps) and with the confocal pinhole, **right** (n=8 sweeps). Both fluorescence traces were filtered to 1 kHz. Under non-confocal conditions we attribute the lower $\Delta F/F$ to the signal from cells and neurites stained with DiO within the culture preparation, but which are not a part of the patch-clamped cell.

Supplementary Figure 7. DiO/DPA AP responses in Purkinje neurons are stable for tens of minutes. A-D, confocal images of the same neuron at different time points showing the change in relative membrane labeling. The laser power and contrast settings were kept identical. The yellow crosses indicate the spot locations where the averaged DiO/DPA responses were measured. **E**, averaged APs (upper traces) recorded at 4 different times relative to the time of DiO labeling. Bottom traces are averaged DiO/DPA responses color coded identical to the electrical recordings. The n-value indicated is the number of sweeps used for each averaged trace.

References

Chanda B, Blunck R, Faria LC, Schweizer FE, Mody I, Bezanilla F (2005) A hybrid approach to measuring electrical activity in genetically specified neurons. Nat Neurosci 8:1619-1626.

Djurisic M, Antic S, Chen WR, Zecevic D (2004) Voltage imaging from dendrites of mitral cells: EPSP attenuation and spike trigger zones. J Neurosci 24:6703-6714.

Dragsten PR, Webb WW (1978) Mechanism of the membrane potential sensitivity of the fluorescent membrane probe merocyanine 540. Biochemistry 17:5228-5240.

Dragsten PR, Blumenthal R, Handler JS (1981) Membrane asymmetry in epithelia: is the tight junction a barrier to diffusion in the plasma membrane? Nature 294:718-722.

Gan WB, Grutzendler J, Wong WT, Wong RO, Lichtman JW (2000) Multicolor "DiOlistic" labeling of the nervous system using lipophilic dye combinations. Neuron 27:219-225.

Kimmich GA, Philo RD, Eddy AA (1977) The effects of ionophores on the fluorescence of the cation 3,3'-dipropyloxadicarbocyanine in the presence of pigeon erythrocytes, erythrocyte 'ghosts' or liposomes. Biochem J 168:81-90.

Melikyan GB, Deriy BN, Ok DC, Cohen FS (1996) Voltage-dependent translocation of R18 and DiI across lipid bilayers leads to fluorescence changes. Biophys J 71:2680-2691.

O'Brien JA, Lummis SC (2006) Diolistic labeling of neuronal cultures and intact tissue using a hand-held gene gun. Nat Protoc 1:1517-1521.

Ratzliff AH, Howard AL, Santhakumar V, Osapay I, Soltesz I (2004) Rapid deletion of mossy cells does not result in a hyperexcitable dentate gyrus: implications for epileptogenesis. J Neurosci 24:2259-2269.

Sengupta P, Holowka D, Baird B (2007) Fluorescence resonance energy transfer between lipid probes detects nanoscopic heterogeneity in the plasma membrane of live cells. Biophys J 92:3564-3574.

Sims PJ, Waggoner AS, Wang CH, Hoffman JF (1974) Studies on the mechanism by which cyanine dyes measure membrane potential in red blood cells and phosphatidylcholine vesicles. Biochemistry 13:3315-3330.

Waggoner A (1976) Optical probes of membrane potential. J Membr Biol 27:317-334.

Supplementary Figure 1

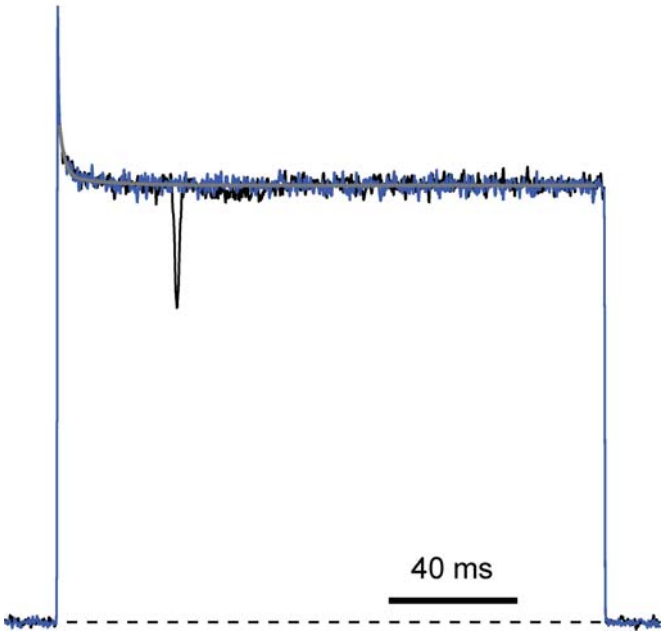

Supplementary Figure 2

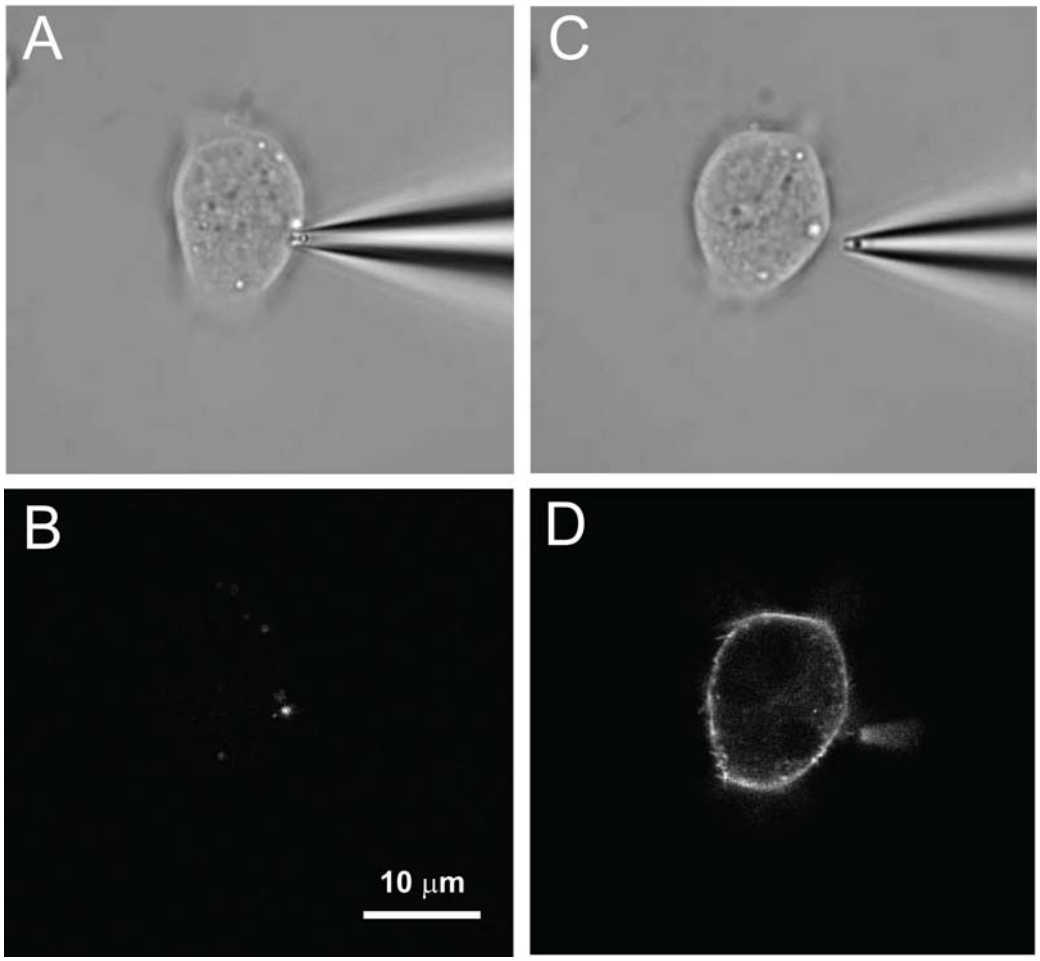

Supplementary Figure 3

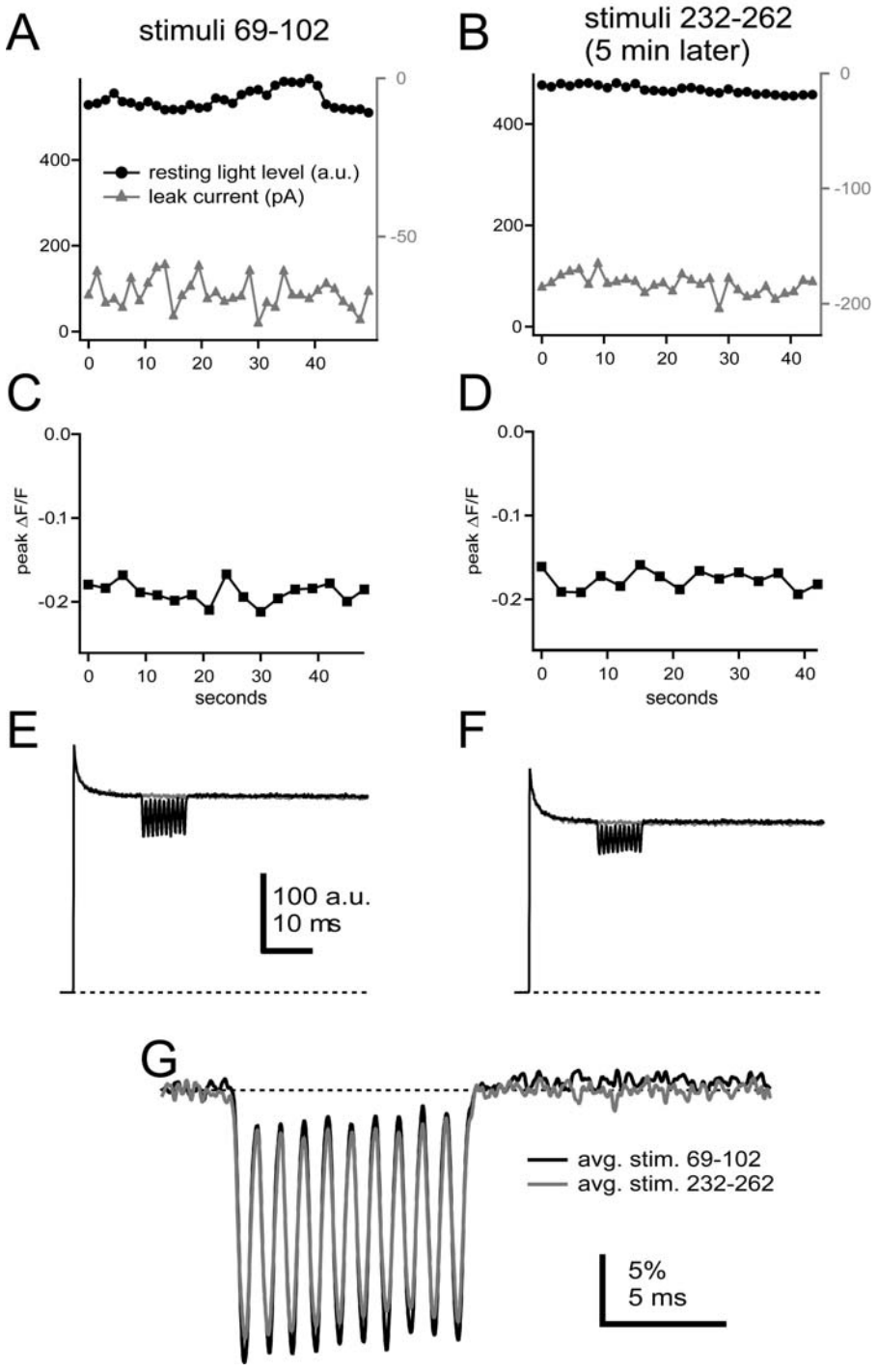

Supplemental Figure 4

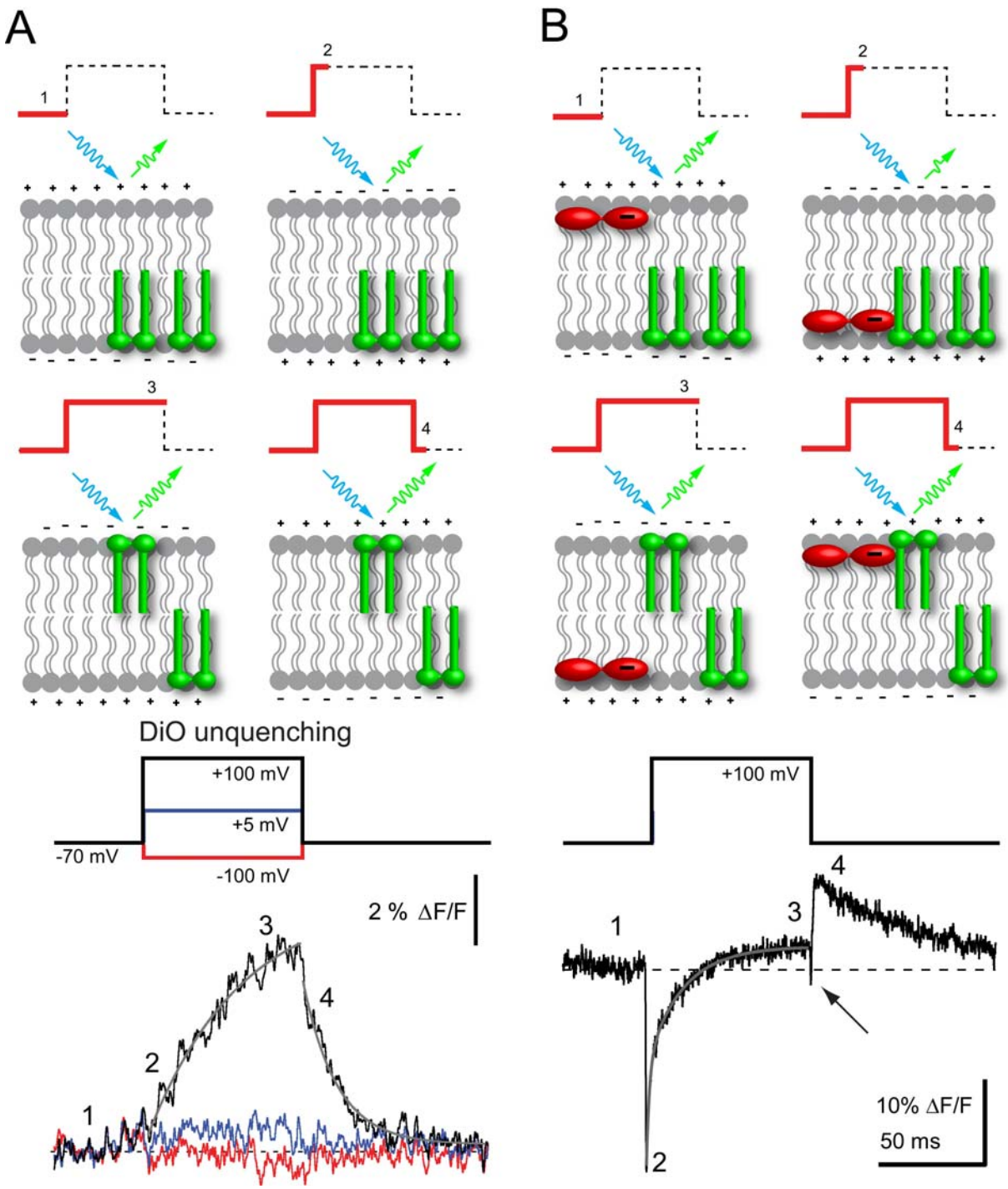

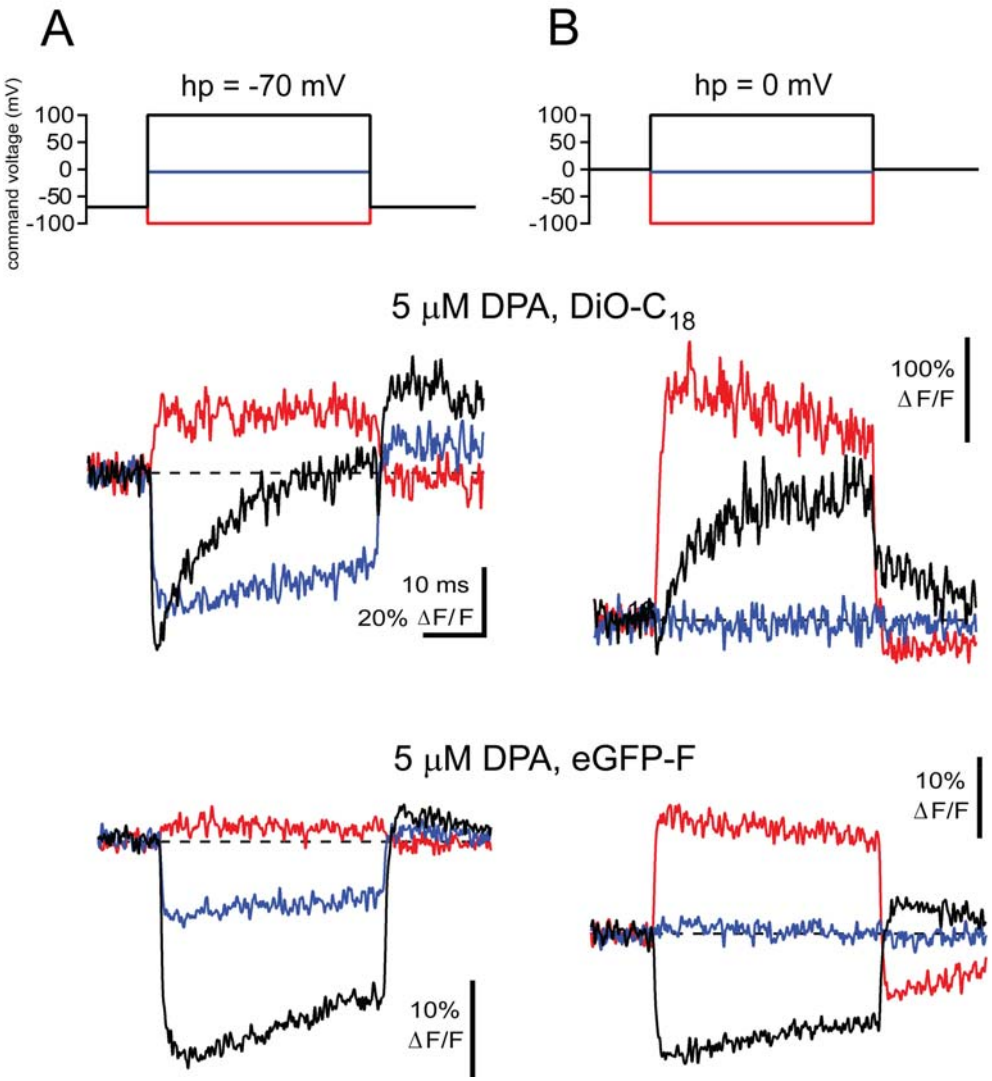
A
B
hp = -70 mV
hp = 0 mV
command voltage (mV)
100
50
0
-50
-100
5 μM DPA, DiO-C18
10 ms
20% ΔF/F
100%
ΔF/F
5 μM DPA, eGFP-F
10%
ΔF/F
10%
ΔF/F

Supplementary Figure 6

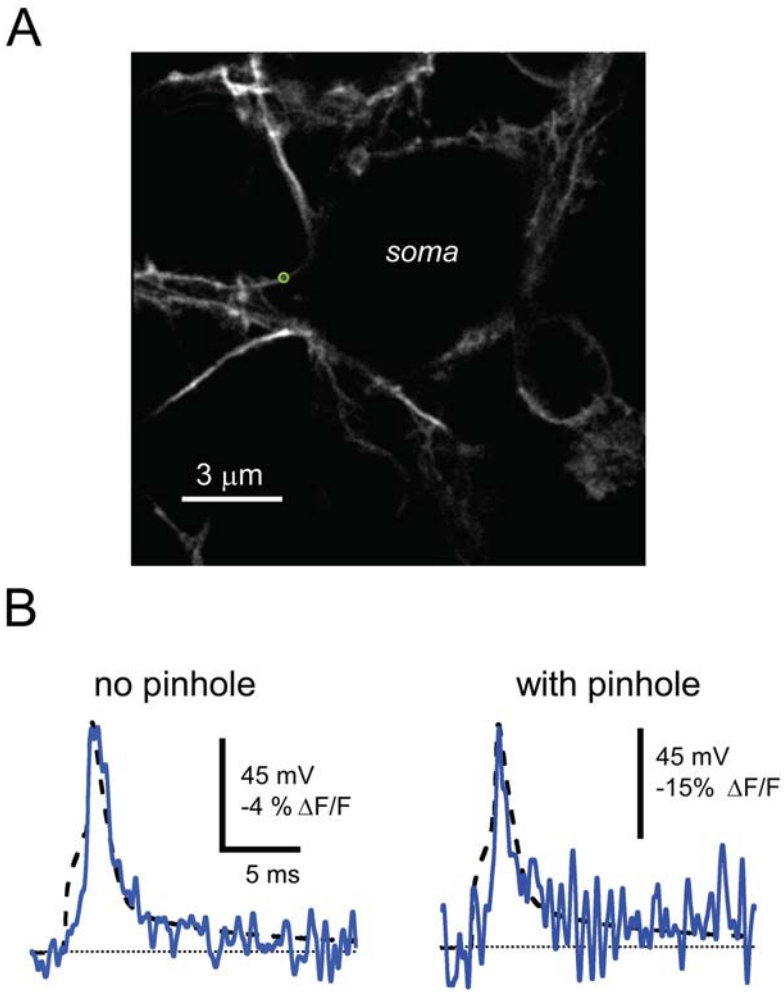

Supplementary Figure 7